

Magnetic properties of Co-Cu metastable solid solution alloys

Xu Fan, Tsutomu Mashimo,* and Xinsheng Huang

Shock Wave and Condensed Matter Research Center, Kumamoto University, Kurokami 2-39-1, Kumamoto 860-8555, Japan

Tomoko Kagayama and Akira Chiba

Faculty of Engineering, Kumamoto University, Kurokami 2-39-1, Kumamoto 860-8555, Japan

Keiichi Koyama and Mitsuhiro Motokawa

Institute for Materials Research, Tohoku University, Sendai 980-8677, Japan

(Received 31 March 2003; revised manuscript received 20 November 2003; published 26 March 2004)

Metastable solid solution alloy powders and bulk alloys in the cobalt(Co)-copper(Cu) (10–90 mol % Co) system, which is an almost immiscible system at the ambient state, were prepared by mechanical alloying (MA) and shock compression. All MA-treated powders showed the x-ray diffraction patterns of a single phase of fcc structure. The lattice parameter increases with Cu concentration and is fundamentally on the line with Vegard's law. The magnetization curves of $\text{Co}_x\text{Cu}_{100-x}$ ($x=20-80$) metastable bulk alloys at room temperature showed ferromagnetism, while the one of $\text{Co}_{10}\text{Cu}_{90}$ system showed paramagnetism. The saturation magnetic moment (M_s) curve versus electron numbers per atom at 0 K was found to be similar to the Slater-Pauling curves of other transition-metal binary systems and decreased with increasing Cu concentration and approached zero at about 28.8 electrons per atom. The magnetoresistance ratio at room temperature increased with Cu content in the ferromagnetic region, while the one of the paramagnetic $\text{Co}_{10}\text{Cu}_{90}$ alloy was negligibly small.

DOI: 10.1103/PhysRevB.69.094432

PACS number(s): 61.66.-f, 61.72.Ff

I. INTRODUCTION

The equilibrium phase diagram of the Co-Cu system¹ shows virtually no solubility of Co in Cu or Cu in Co below 500 °C. Therefore, the physical properties of the solid solution in the Co-Cu system are not well known yet. For example, the Slater-Pauling curve does not include the data of this system. In addition, since the observation of giant magnetoresistance (GMR), this system has become a model system for studying GMR.

Several works have been done to produce the metastable solid solution in the Co-Cu system. Kneller² reported many years ago that Co-Cu films evaporated at room temperature formed metastable fcc solid solutions. Gente *et al.*³ and Huang *et al.*⁴ have prepared Co-Cu solid solution alloys by mechanical alloying (MA). Recently a great deal of attention has been focused on GMR in the Co-Cu system. In the literature, nanoscaled granular Co-Cu system alloys prepared by the sputtering method,⁵⁻⁷ repeated rolling method,⁸ melt-spinning,^{9,10} and MA¹¹⁻¹⁵ have been found to exhibit GMR effects, by annealing at an opportune temperature. On the other hand, magnetoresistance (MR) measurement of the Co-Cu system solid solution has not been reported yet. The magnetization measurements at low temperature of the Co-Cu system solid solution are also still lacking, although the thin-film samples obtained by magnetron sputtering have been investigated by Childress and Chien.

The MA has recently been used to prepare amorphous phases, metastable solid solution phases, nanocrystalline phases, high-pressure phases, and so on. It is important to consolidate these powders for evaluating physical properties and for applications. On the other hand, shock compression can be used as an effective consolidation method for meta-

stable material powders without recrystallization or decomposition.¹⁶⁻²¹ We have prepared nonequilibrium bulk alloys, including metastable solid solution, amorphous phase, nanocrystals in W-Cu,¹⁷ Fe-Cu,¹⁸ Fe-W,¹⁹ Fe-Co,²⁰ etc., systems by using the MA and shock compression. Particularly, the magnetization results of the Fe-Cu solid solutions showed a fit curve to the Slater-Pauling one.²¹ In this study, we prepared bulk bodies of metastable solid solution alloy in the Co-Cu system to study the magnetization and magnetoresistance.

II. EXPERIMENT

Starting powders were provided by Rare Metallic Co., Ltd. The Co and Cu powders consisted of irregular particles of 1–2 μm and 325 mesh ($<44 \mu\text{m}$) in diameter, and the purities of Co and Cu in the catalog were 99.9 and 99.99 wt %, respectively. The MA experiments were carried out by using the planetary micro ball mill (P-7 of Fritsch Co., Ltd.) in an argon atmosphere glove box.¹⁶ A mill capsule with an inner diameter of 41 mm and a depth of 38 mm and balls with a diameter of 5 mm were used, which were made of silicon nitride (Si_3N_4) and zirconia (Y_2O_3 -doped tetragonal ZrO_2), respectively. The starting powder with a weight of 20 g and 200 zirconia balls were contained into the capsule with a ball-to-powder weight ratio of about 4:1. The rotation speed of the ball mill was 2840 rpm. The milling was interrupted each 30 min for 35 min to cool the mill capsule to avoid heating. The milling duration was 3 h, and a small amount of the material was taken for analysis after selected milling times.

Shock compression recovery experiments were conducted using a propellant gun.^{22,23} The MA-treated powder specimens were enclosed in a brass (Cu:Zn=70:30 in wt %) cap-

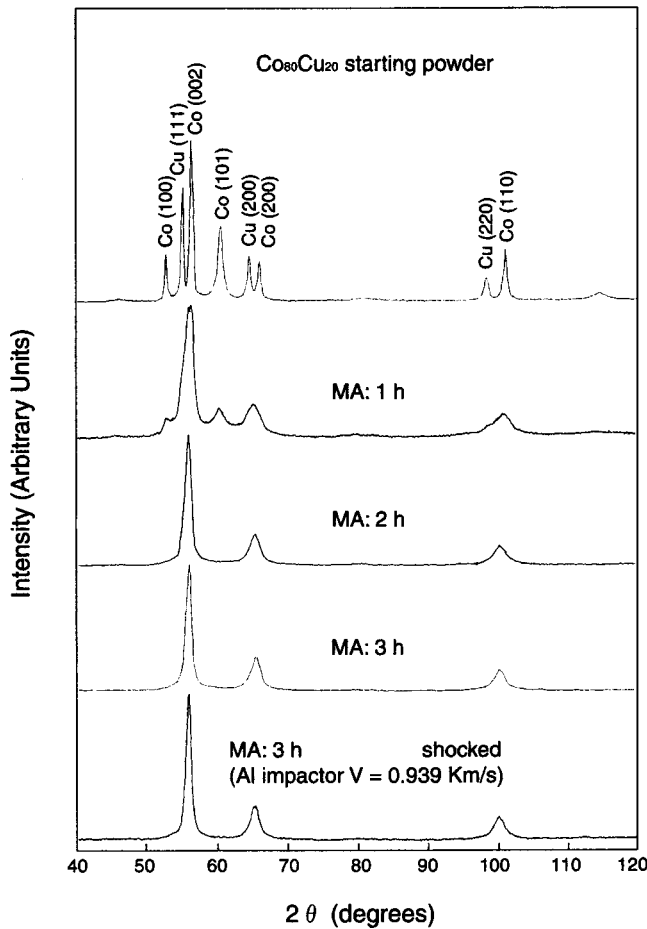


FIG. 1. XRD patterns of the starting powder, the MA-treated powders, and the shock-consolidated bulk body in the $\text{Co}_{80}\text{Cu}_{20}$ system.

sule with an inside diameter of 12 mm and with an inside height of 4–5.6 mm. The porosities of pellets were 45%–54%. Shock loading was carried out by impacting the capsule with an aluminum alloy (2024Al) flat flyer plate whose thickness was about 3 mm. The MA-treated and shock-consolidated specimens were investigated by powder x-ray diffraction (XRD), instrumental chemical analysis, and electron probe microanalysis (EPMA).

Magnetization curves at room temperature of the metastable bulk alloys were measured by a vibrating sample magnetometer (VSM) apparatus combined with a conventional magnet (Riken Denshi Co., Ltd. BHV-30HT, whose maximum magnetic field is 15 kOe) up to 10 kOe. The magnetization measurements at liquid helium temperature (4 K) were carried out using a VSM apparatus combined with a superconducting magnet (Oxford Instruments, Mag. Lab. VSM, whose maximum magnetic field is 150 kOe) in applied fields up to 130 kOe, and saturation magnetic moments at 0 K were obtained by extrapolation method. Magnetoresistance (MR) at room temperature was measured using a dc four-probe method by a R6581 Digital Multimeter (Advantest Co., Ltd.) apparatus combined with a conventional magnet (Riken Denshi Co., Ltd. BHV-30HT, whose maximum magnetic field is 15 kOe) under a magnetic field up to

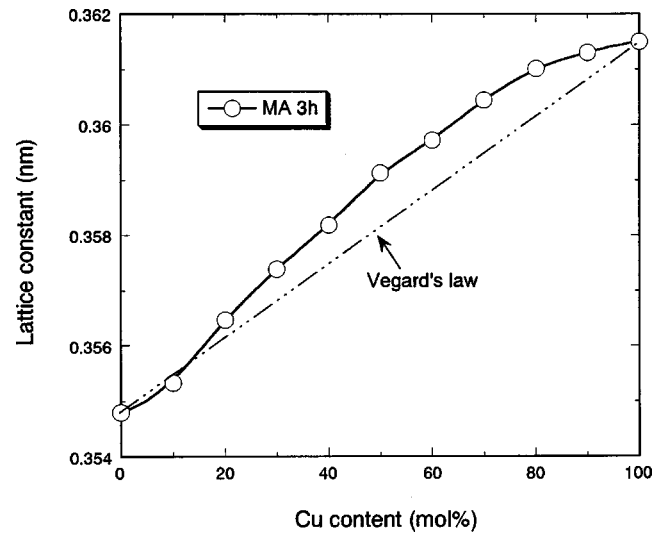


FIG. 2. Lattice parameter vs Cu concentration of MA-treated (3 h) $\text{Co}_x\text{Cu}_{100-x}$ ($x=10-90$) solid solutions.

7 kOe. We used rectangular bulk samples that had length, width, and thickness of about 10, 3, and 1–2 mm, respectively. The MR ratio was calculated as the absolute value of $\Delta\rho/\rho_0 = (\rho_H - \rho_0)/\rho_0$, where ρ_0 is the resistivity at zero field and ρ_H is the resistivity at the applied field of H .

III. RESULTS AND DISCUSSION

A. Metastable solid solution alloys

The XRD patterns of the starting powder and MA-treated powders in the $\text{Co}_{80}\text{Cu}_{20}$ system are shown in Fig. 1. Even after 2 h of milling, the Co peaks have fully disappeared, and only the broad peaks of the fcc phase can be observed. The fcc phase peaks were observed on higher-angle side than the peaks of pure Cu. Similar results were obtained for all other samples. The lattice constants estimated from the diffraction peaks of fcc phase powders for 3 h of MA treatment are shown in Fig. 2. The lattice parameters of MA-treated powders were smaller than that of pure Cu, and were larger than that of pure Co respectively. It was found that the lattice parameter increases with Cu content and is fundamentally in the line with Vegard's law, which shows that the supersaturated solid solution was formed in the Co concentration range of 10–90 mol %. However, the lattice parameters also showed a little positive deviation from Vegard's law, which may be due to the magnetovolumetric effect.

Many works^{24–28} showed that small Co-rich clusters are still present, even after long milling times. So we cannot rule out an inhomogeneous distribution of Co in the Cu matrix. We prepared Fe-Cu system alloys, almost a consisting of supersaturated solid solution, by MA treatment earlier. Since the enthalpy of mixing²⁹ ($H_{\text{mix}} = +13$ kJ/g atom) for $\text{Fe}_{50}\text{Cu}_{50}$ system is much larger than that of the $\text{Co}_{50}\text{Cu}_{50}$ system³ ($H_{\text{mix}} = +6$ kJ/g atom), it may be easy to prepare solid solution for the Co-Cu system compared with the Fe-Cu system. So we concluded that the MA-treated Co-Cu samples in this study almost all consisted of solid solution.

TABLE I. Chemical analytical results for zirconium, silicon, carbon, oxygen, and nitrogen contents.^a

Chemical element		Zr ^b (wt %)	Si ^b (wt %)	O ^c (wt %)	N ^d (wt %)	C ^e (wt %)
Starting	Co	<0.001	0.001	1.06	0.01	0.001
Powder	Cu	<0.01	<0.01	1.23	0.01	0.33
Co:Cu=80:20 (in mol %)	MA-treated (3 h)	0.42	0.019	1.92	0.06	0.12
	Shock-consolidated			2.17	0.07	0.20
Co:Cu=50:50 (in mol %)	MA-treated (3 h)	0.80	0.022	1.57	0.10	0.21
Co:Cu=20:80 (in mol %)	MA-treated (3 h)	0.38	0.024	1.53	0.12	0.32

^aThe measurement errors for silicon, nitrogen, oxygen, and carbon content were less than 0.0001, 0.07, 0.02, and 0.01 wt %, respectively.

^bMeasured by inductively coupled argon plasma emission spectrophotometry with the SPS-1200 of Seiko Electric Co., Ltd.

^cMeasured by the combustion in oxygen nondispersive infrared absorption method with the LECO Corp. TC-436.

^dMeasured by the inert-gas fusion thermal conductivity method with the LECO Corp. TC-436.

^eMeasured by the inert-gas fusion thermal conductivity method with the LECO Corp. WR-112.

A series of fcc solid solution bulk bodies, whose diameter is about 12 mm and thickness is about 2.5 mm, were prepared by shock compression of MA-treated (3 h) powders in the Co-Cu system. No large crack could be observed, and the cross sections showed a metallic gloss. The morphology appeared almost as a uniform single phase over the entire surface. The EPMA results showed that Co and Cu dispersed well at the submicron level in shock-consolidated bulk bodies. The XRD pattern of shock-consolidated bulk bodies in the Co₈₀Cu₂₀ system formed at an impact velocity of 0.939 km/s did not change much from that of the MA-treated powder, as shown in Fig. 1. This showed that the metastable solid solution powder was successfully consolidated without decomposition or recrystallization.

The chemical analytical results of Zr, Si, O, N, and C in the starting powder, the MA-treated (3 h) powders in Co₈₀Cu₂₀, Co₅₀Cu₅₀, and Co₂₀Cu₈₀ systems, and Co₈₀Cu₂₀ shock-consolidated bulk body are summarized in Table I. It was found that the impurity contents of the MA-treated powders and bulk body were much higher than those of the starting powder and the O, N, and C content did not much change by shock compression of the Co₈₀Cu₂₀ bulk body. The Zr, Si, and N contents in the MA-treated powders all increased from those of the starting powders (all <0.01 wt %) due to wear debris from zirconia balls and silicon nitride mill capsule. The O content may be due to the wear debris from the zirconia balls, the O content of the Co (1.06 wt %) and Cu (1.23 wt %) starting powder, and oxidation occurred during the MA treatment. However, the XRD peaks of oxide cannot be detected. The average total impurity content of Zr, Si, O, N, and C in the MA-treated powders was calculated to about 2.5 wt %. These impurities would not very much disturb the magnetic property of the metastable bulk samples, because they are nonmagnetic materials.

B. Magnetic properties

Figure 3 shows the magnetization curve (up to 10 kOe) at room temperature of the fcc metastable bulk alloys. The

magnetization curves of Co₈₀Cu₂₀, Co₅₀Cu₅₀, and Co₂₀Cu₈₀ bulk samples show hysteresis loops, which indicates that they are ferromagnetic. On the other hand, one of the Co₁₀Cu₉₀ systems almosts shows a straight line: the magnetization of about 0.07 kG under a field of 10 kOe and the coercivity of about 0.06 kOe are too small, which means that it is paramagnetic.

To determine the saturation magnetic moments at 0 K for discussing the Slater-Pauling curve, at first, the magnetizations were measured at 4 K by using a superconducting magnet up to 130 kOe and then decreased to 100 kOe in order to

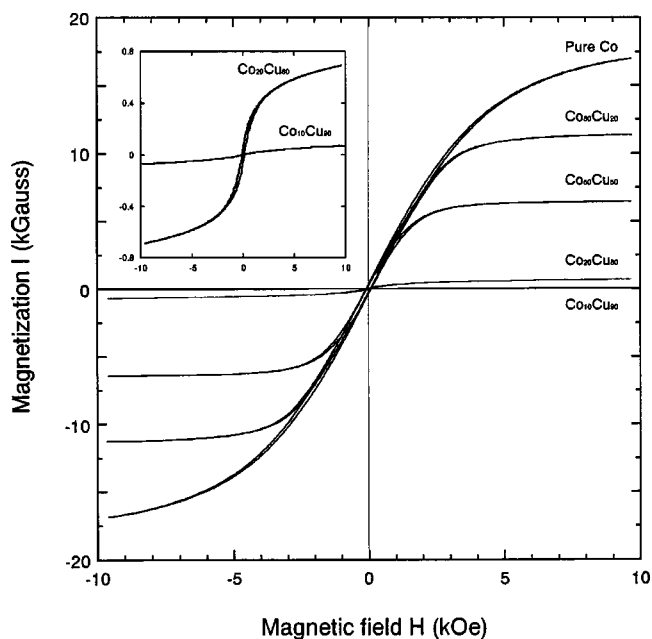
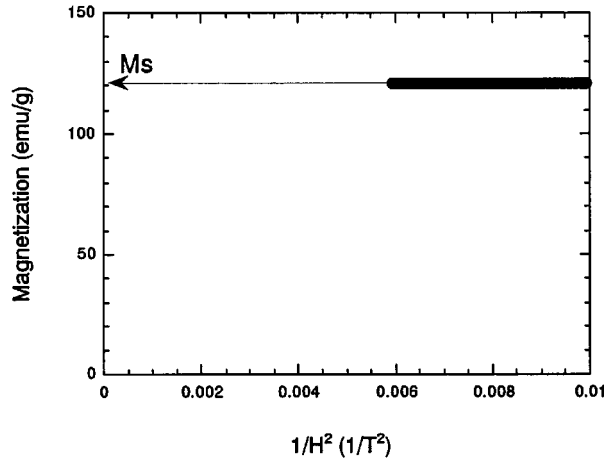


FIG. 3. Magnetization curves up to 10 kOe at room temperature of the Co_xCu_{100-x} ($x=100, 80, 50, 20,$ and 10) metastable bulk alloys obtained from 3-h MA-treated powders.

a) Magnetization - $1/H^2$ 

b) Magnetization - temperature

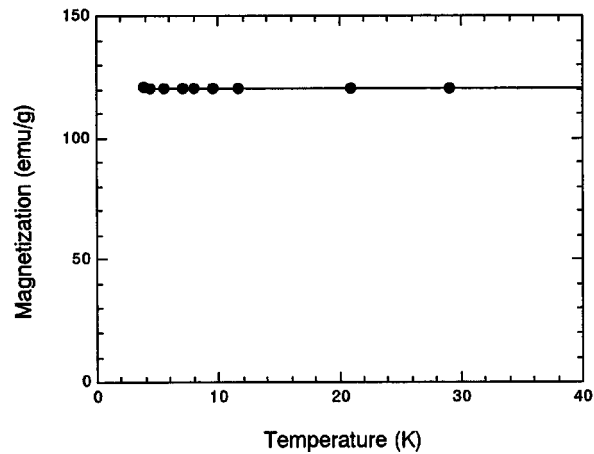


FIG. 4. Magnetization measurement results up to 130 kOe at low temperature of the fcc metastable $\text{Co}_{80}\text{Cu}_{20}$ bulk alloy. (a) Magnetization curve vs $1/H^2$ at 4 K. (b) Magnetization curve vs temperature at 100 kOe.

obtain the saturation magnetization at 4 K. After that, the relationship of magnetization and temperature was measured by increasing the temperature from 4 K to room temperature with the magnetic field kept at 100 kOe. The samples of metastable bulk alloys in the Co-Cu system used in magnetization measurements were prepared by cutting as quasicubic forms [about $3 \times 3 \times (2-3)$ mm]. The magnetizations were calibrated by pure nickel (Ni) metal with a quasicubic form of $3 \times 3 \times 3$ mm, and a reported value [58.57 emu/g (Ref. 30)] of saturation magnetization at 4 K was used in the magnetization calibration. Figure 4 shows a typical magnetization measurement result of $\text{Co}_{80}\text{Cu}_{20}$ metastable bulk alloy. The saturation magnetization (I_s) at 4 K of the sample was determined from extrapolation of the magnetization (I) versus $1/H^2$ (H : the magnetic field) curve to as infinite field, as shown in Fig. 4(a). And then the I_s at 0 K was obtained by extrapolating the I_s data at 4 K using the gradient [as shown in Fig. 4(b)] of I versus temperature at 100 kOe. The I_s values were corrected by considering the average total impurity content mentioned above.

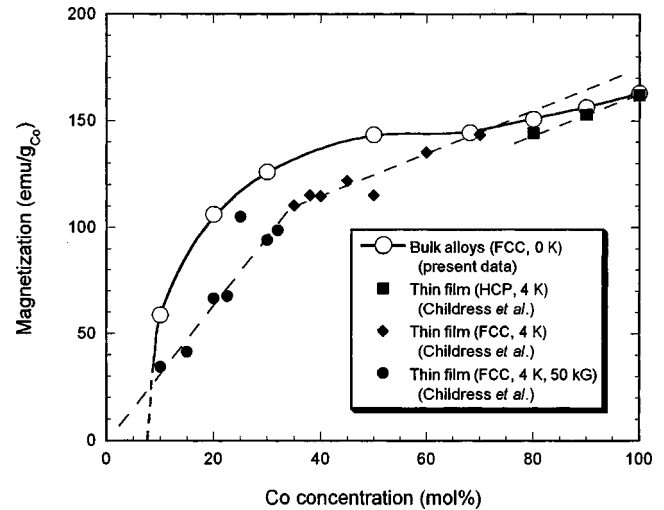


FIG. 5. Saturation magnetization of the bulk alloys at 0 K (present data) and the results of thin films (prepared by magnetron sputtering) obtained at 4 K by Childress and Chien units of emu per gram of Co vs Co concentration. The dashed line was drawn by fitting the measured data to a quadratic curve with the least squares method.

Figure 5 shows the saturation magnetization of the Co-Cu system bulk alloys at 0 K (present data) and the results of thin films (prepared by magnetron sputtering) obtained at 4 K by Childress and Chien⁵ in units of emu per gram of Co versus Co concentration. Comparing our results with those data, the magnetization of the thin-film sample almost shows three unconnected straight lines and first decreases slightly with Cu content up to 70 mol %, then decreases rapidly and tends to zero at 100 mol % Cu. But the present data show a smooth and continuous curve, and approach zero at 92 mol % Cu. Such a change of magnetization also shows that the supersaturated solid solution was formed by MA treatment.

Figure 6 shows the saturation magnetic moment (M_s) at 0 K of the metastable bulk alloys in the Co-Cu system per atom (Bohr magneton) versus the number of electrons. The black circle points are the data in Fe-Cu system²¹ data measured by the same method. The black square points are the present data. The M_s values at 0 K decreased with Cu concentration and approached zero at about 90 mol % Cu (28.8 electrons per atom) content like the Slater-Pauling curves of the other alloys. This result was consistent with the hysteresis loop result (Fig. 3).

Figure 7 shows the magnetoresistance (MR) measurement result obtained at room temperature under a magnetic field applied parallel to the current up to 7 kOe for $\text{Co}_{80}\text{Cu}_{20}$, $\text{Co}_{50}\text{Cu}_{50}$, $\text{Co}_{30}\text{Cu}_{70}$, and $\text{Co}_{10}\text{Cu}_{90}$ bulk alloys. In addition, magnetization curves are also plotted up to 7 kOe in this figure to help to understand the MR effect. The MR ratio increased with Cu content in the ferromagnetic range, and the maximum value was 1.38% for $\text{Co}_{30}\text{Cu}_{70}$ bulk alloy. But the MR ratio of $\text{Co}_{10}\text{Cu}_{90}$ bulk alloy was negligibly small. This may be due to the paramagnetism of this alloy indicated by the magnetization measurement results. This is supported by the fact that the bulk alloys prepared in this study almost consisted of solid solution and provided a figure

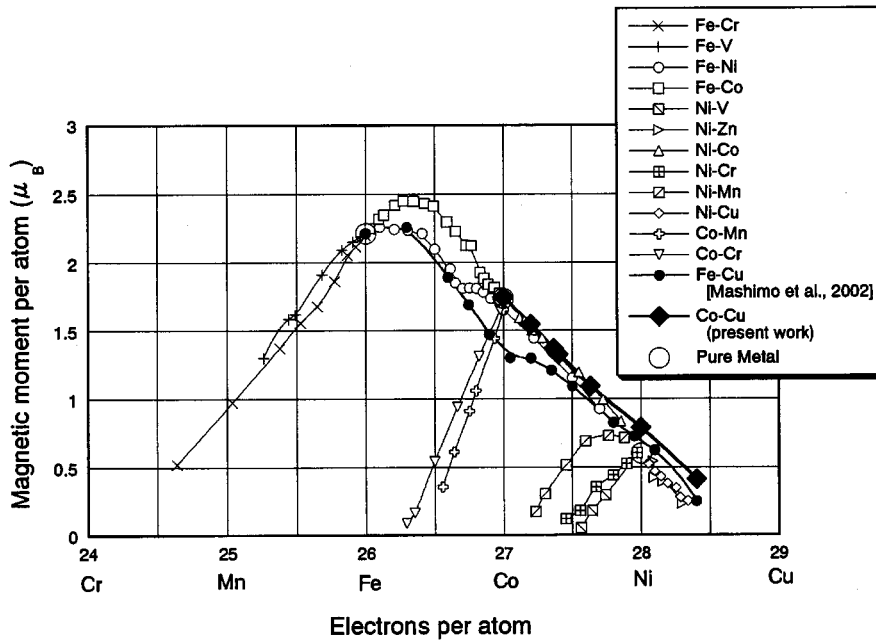


FIG. 6. Saturation magnetic moment per atom vs the number of electrons per atom at 0 K of the transition metals and their alloys (Slater-Pauling curve).

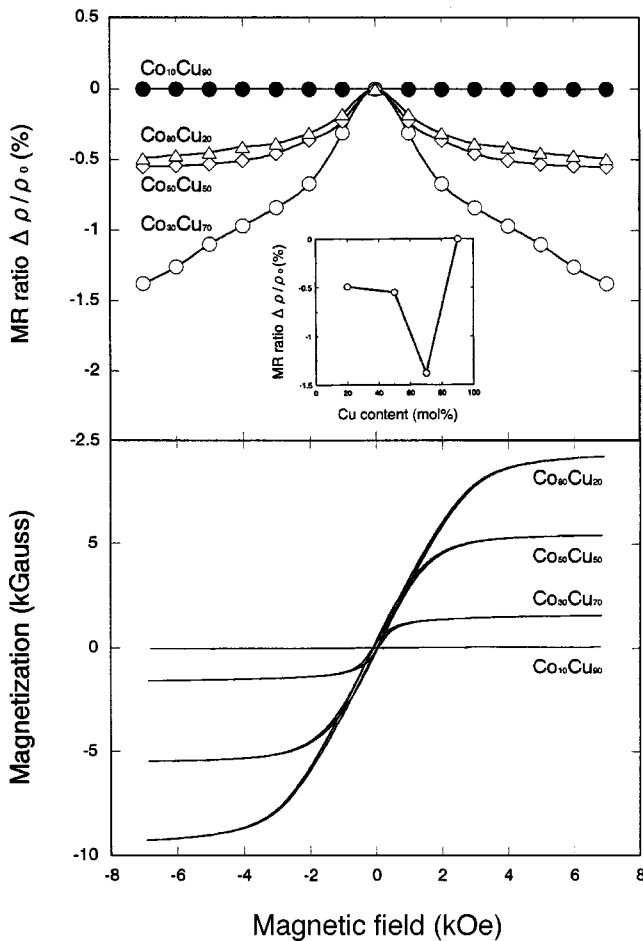


FIG. 7. Magnetoresistance (MR) and magnetization measurement results up to 7 kOe at room temperature of Co_xCu_{100-x} metastable bulk alloys.

of a fundamental magnetic property of the Co-Cu system. In addition, the MR ratios obtained under a magnetic field perpendicular to the current are almost as big as the above data and show isotropy. The MR values of the ferromagnetic Co-Cu alloys are much smaller than those of the annealed samples.^{9,12} The MR effect of the Co-Cu alloy in the ferromagnetic range is generally attributed to spin-dependent scattering in the Co magnetic fine particles diluted in a non-magnetic Cu phase. The value of the MR ratio depends on the precipitated grain size, the distribution of the particles, and the microstructure.

Childress and Chien⁵ found that Co-Cu alloys exhibit a spin glass transition below 40 K for low Co concentration (below 23 mol %) and show coexistence of both spin glass and ferromagnetic behavior for Co concentration from 24 to 40 mol %. In this work, we did not measure the changes of zero-field-cooled and field-cooled (with a small field) magnetization, while we measured the magnetization changes with temperature under high a field of 100 kOe. No magnetic effect is observed in the low-temperature range of 10–50 K, so the effect of spin glasses on magnetization under a large magnetic field could be negligible, even though there maybe a small part of the samples involved in the spin glass transition.

IV. CONCLUSION

In this study, only fcc phase peaks were observed in the XRD patterns of MA-treated powder, and the lattice parameter is almost in the line with Vegard’s law. In addition, the saturation magnetization at 0 K shows a smooth and continuous curve, and approaches zero at about 90 mol % Cu. Based on the results presented above, we concluded that the Co-Cu system bulk alloys prepared by mechanical alloying and shock compression almost consist of supersaturated solid solution. The magnetization measurement result at room temperature indicates that the metastable bulk alloys are ferro-

magnetic in the Cu content regions of 0–80 mol %, while the $\text{Cu}_{10}\text{Cu}_{90}$ system alloy exhibits paramagnetic behavior. The saturation moment calculation result at 0 K is consistent with the Slater-Pauling curve of other binary alloy systems. We expect that the present data will offer useful information for discussion of the magnetism of transition-metal alloys. The MR ratio of $\text{Co}_{10}\text{Cu}_{90}$ alloy was negligibly small although the one in $\text{Co}_{80}\text{Cu}_{20}$, $\text{Co}_{50}\text{Cu}_{50}$, and $\text{Co}_{30}\text{Cu}_{70}$ alloys increased with Cu content. This result also indicated that $\text{Co}_{10}\text{Cu}_{90}$ alloy was paramagnetic and was consistent with

the magnetization results. The MR ratio of the annealed Co-Cu bulk alloys is now under study.

ACKNOWLEDGMENTS

The authors would like to thank Japan New Metals Co., Ltd. for their support in the instrumental chemical analyses. A part of work was carried out at the High Field Laboratory for Superconducting Materials, Institute for Materials Research, Tohoku University. This work was supported in part by the 21st century COE program of Pulsed Power Science.

*Corresponding author. Fax: +81-96-342-3293. Electronic address: mashimo@gpo.kumamoto-u.ac.jp

¹T. Nishizawa and K. Ishida, *Bull. Alloy Phase Diagrams* **5**, 161 (1984).

²E. Kneller, *J. Appl. Phys.* **33S**, 1355 (1962).

³C. Gente, M. Oehring, and R. Bormann, *Phys. Rev. B* **48**, 13244 (1993).

⁴J. Y. Huang, Y. D. Yu, Y. K. Wu, D. X. Li, and H. Q. Ye, *J. Mater. Res.* **12**, 936 (1997).

⁵J. R. Childress and C. L. Chien, *Phys. Rev. B* **43**, 8089 (1991).

⁶A. E. Berkowitz, J. R. Mitchell, M. J. Carey, A. P. Young, S. Zhang, F. E. Spada, F. T. Parker, A. Hutten, and G. Thomas, *Phys. Rev. Lett.* **68**, 3745 (1992).

⁷John Q. Xiao, J. Samuel Jiang, and C. L. Chien, *Phys. Rev. Lett.* **68**, 3749 (1992).

⁸K. N. Ishihara, T. Matsumoto, A. Ohtsuki, and P. H. Shingu, *Solid State Phenom.* **42-43**, 77 (1995).

⁹X. Song, S. W. Mahon, B. J. Hickey, M. A. Howson, and R. F. Cochrane, *Mater. Sci. Forum* **225-227**, 163 (1996).

¹⁰E. Agostinelli, P. Allia, R. Caciuffo, D. Fiorani, D. Rinaldi, A. M. Testa, P. Tiberto, and F. Vinai, *Mater. Sci. Forum* **235-238**, 705 (1997).

¹¹Y. Ueda and S. Ikeda, *Mater. Trans., JIM* **36**, 384 (1995).

¹²Y. Ueda, S. Ikeda, and S. Chikazawa, *Jpn. J. Appl. Phys., Part 1* **35**, 3414 (1996).

¹³A. Y. Yermakov, M. A. Uimin, A. V. Shangurov, A. V. Zarubin, Y. V. Chechetkin, A. K. Shtolz, V. V. Kondratyev, G. N. Konygin, Y. P. Yelsukov, S. Enzo, P. P. Macri, R. Frattini, and N. Cowlam, *Mater. Sci. Forum* **225-227**, 147 (1996).

¹⁴S. W. Mahon, X. Song, M. A. Howson, B. J. Hickey, and R. F. Cochrane, *Mater. Sci. Forum* **225-227**, 157 (1996).

¹⁵Y. G. Yoo, S. C. Yu, and W. T. Kim, *Mater. Sci. Eng., A* **304-306**, 928 (2001).

¹⁶T. Mashimo, S. Tashiro, S. Hirose, and K. Makita, *J. Appl. Phys.* **80**, 356 (1996).

¹⁷T. Mashimo, X. S. Huang, and S. Tashiro, *J. Mater. Sci. Lett.* **16**, 1051 (1997).

¹⁸X. S. Huang and T. Mashimo, *J. Alloys Compd.* **288**, 299 (1999).

¹⁹X. S. Huang and T. Mashimo, *J. Alloys Compd.* **296**, 183 (2000).

²⁰T. Mashimo, X. Fan, X. S. Huang, H. Murata, and M. Sakakibara, *J. Phys.: Condens. Matter* **14**, 10825 (2002).

²¹T. Mashimo, X. S. Huang, X. Fan, K. Koyama, and M. Motokawa, *Phys. Rev. B* **66**, 132407 (2002).

²²T. Mashimo and S. Tashiro, *J. Mater. Sci. Lett.* **13**, 174 (1994).

²³T. Mashimo, S. Ozaki, and K. Nagayama, *Rev. Sci. Instrum.* **55**, 226 (1984).

²⁴R. Elkalkouli, R. Morel, and J. F. Dinhut, *Nanostruct. Mater.* **8**, 313 (1997).

²⁵M. A. Uimin, A. Ye. Yermakov, V. V. Serikov, A. Yu. Korobeinikov, and A. K. Shtolz, *Phys. Status Solidi A* **165**, 337 (1998).

²⁶I. W. Modder, E. Schoonderwaldt, G. F. Zhou, and H. Bakker, *Physica B* **245**, 363 (1998).

²⁷V. A. Ivchenko, M. A. Uimin, A. Ye. Yermakov, and A. Yu. Korobeinikov, *Surf. Sci.* **440**, 420 (1999).

²⁸Y. G. Yoo, D. S. Yang, S. C. Yu, W. T. Kim, and J. M. Lee, *J. Magn. Magn. Mater.* **203**, 193 (1999).

²⁹A. R. Miedema, *Philips Tech. Rev.* **36**, 217 (1976).

³⁰H. Danan, A. Herr, and A. J. P. Meyer, *J. Appl. Phys.* **39**, 669 (1968).